Long and Short Chains in a Polymeric Brush: A Conformational Transition

Aleksander M. Skvortsov

Chemical-Pharmaceutical Institute, Popova 14, 197022 St. Petersburg, Russia

Leonid I. Klushin*

Institute for Macromolecular Compounds of the Russian Academy of Sciences, Bolshoi pr. 31, 199004 St. Petersburg, Russia

Aleksey A. Gorbunov

Research Institute for Highly Pure Biopreparations, Pudozhskaya 7, 197110, St. Petersburg, Russia

Received July 26, 1996; Revised Manuscript Received November 25, 1996[⊗]

ABSTRACT: End-anchored macromolecules admixed to a homogeneous monodisperse planar brush and differing from the majority brush-forming chains only by molecular mass take three different types of conformation, depending on its polymerization index, K, relative to that of the majority chains, N. The fraction of the admixed macromolecules is taken to be small. Shorter minority chains form slightly deformed random coils with both the average end height and its fluctuation proportional to $K^{1/2}$. A longer minority chain with $K > N$ acquires an inhomogeneous flower-like conformation: an N-segment stem of height H equal to the thickness of the brush and a randomly coiled crown outside the brush. The stem is strongly stretched and fluctuates only weakly. The transition from one type of conformation to another occurs as the number of segments of the minority chain, K, changes within a narrow range around N, where the chain is simultaneously strongly stretched and strongly fluctuating. We show that the coil-to-flower transition has some features of both the first- and the second-order phase transitions.

I. Introduction

Polymer chains attached by one end to a surface or a liquid−liquid interface with a high enough anchoring density form a brush. Wide technological applications of polymer brushes (surface modification, stabilization of colloids, etc.) and their importance in helping to understand some fundamental problems of polymeric materials (self-organization in block−copolymer melts, micelle formation, etc.) were the reasons for these systems to attract considerable interest both from experimental and theoretical points of view. A rather good understanding of different aspects of equilibrium and, to a lesser extent, the dynamic behavior of these systems has been achieved by now.[1−4] The existing analytical self-consistent field theory gives a detailed description of the equilibrium brush properties and is widely used in interpreting experimental data. Most analytical results are obtained for strictly monodisperse brushes formed by identical macromolecules. A more general approach valid for polydisperse brushes does not give much insight since it involves numerical solving of integral equations.[5]

The simplest case of a polydisperse brush is obtained by mixing two monodisperse fractions. This system was studied in detail in refs 5 and 6. The main result is that the brush segregates into two sublayers and the chains belonging to each fraction are stretched, their end-to-end distance being proportional to their respective contour length. Chain stretching is caused by crowding. In the lower sublayer the neighboring chains of both species have to overlap, while in the second sublayer only the upper parts of the longer chains are interacting with each other. The approach used is only valid under the condition of strong overlapping for both species separately, $N_1\rho_1 \gg 1$, $N_2\rho_2 \gg 1$, where N_1 and N_2 are the segment numbers for the shorter and longer species, and ρ_1 and ρ_2 are the respective grafting densities.

When one of the species does not satisfy this condition, the situation is quite different. If the minority chains are shorter ($N_1 < N_2$), their conformation is that of a weakly deformed coil[7] with the average size of order $N_1^{1/2}$. The closer N_1 is to N_2, the stronger is the deformation: under the condition that $\lambda = 1 - N_1/N_2 \ll 1$, both the size and its average fluctuation for a minority chain increases dramatically as $\lambda^{-1/2}$ until they saturate at the values for the monodisperse brush formed by the majority species. On the other hand, it is natural to assume that in the case of $N_1 > N_2$, the long minority chains should acquire a flower-like inhomogeneous conformation with a stretched stem and a coiled crown;[7] see Figure 1.

The aim of the present paper is to investigate the properties of the flower conformation and to follow the entire transition in the conformation of the minority chain as its molecular weight changes from low to high values (as compared to that of the majority chains). The approach used is based on the mean-field picture of the brush characterized by the parabolic profile of the chemical potential. The problem of a minority chain in the brush is then reduced to finding the chain conformation in the known external field. If the chemical potential were indeed parabolic over the entire space, the partition function of the chain could be mapped onto the Green's function of the quantum harmonic oscillator. This will be shown to be a valid approximation for the short minority chains that keep inside the brush density profile, but describing the flower conformation of a long chain requires a more elaborate approach. The logic of

* On leave from the American University of Beirut, Department of Physics, Beirut, Lebanon, and author to whom correspondence should be addressed.

[⊗] Abstract published in *Advance ACS Abstracts,* February 1, 1997.

S0024-9297(96)01111-4 CCC: $14.00

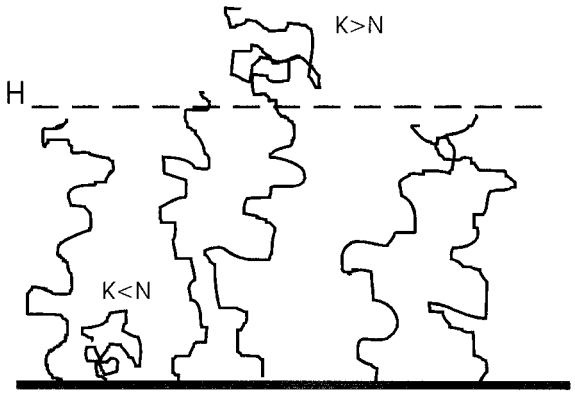

Figure 1. Schematic representation of minority chain conformations in a polymeric brush. The minority chain consists of K segments, the majority chains of N segments. The broken line shows the brush thickness, H. For $K < N$, the chain is in a coil-like conformation; for $K = N$, it is stretched and strongly fluctuates; for $K > N$, it has an inhomogeneous flower-like conformation.

it is as follows: We start by introducing a simplified picture based on neglecting the fluctuations of the stem and assuming that the crown cannot penetrate the inside of the brush. The analytical results for the minority chains are compared to numerical SCF calculations. Then, we describe the fluctuation effects which are especially prominent when the difference between the two species is relatively small. Finally, we discuss the character of the coil-to-flower transition upon increasing the molecular mass of the minority chain included in a given brush and compare it to some other phase transitions in isolated macromolecules.

II. Analytical Description

Consider a brush formed by flexible chains anchored with surface density $\rho = a^2/s$, where s is the surface area per chain and a is the segment length assumed to be equal to the chain thickness. We take a as the unit length and omit it in the subsequent formulas. The brush is immersed in a good solvent. To simplify the notation, we denote by N and K the number of segments in a majority chain and minority chain, respectively. It is worth stressing once again that when the brush is formed by chains of two species which differ in their molecular mass, two regimes exist. If the chains of each species overlap strongly, a segregated bidisperse brush is formed where all macromolecules are considerably stretched.[5,6] We are studying another regime where the minority chains do not feel each other. Then their conformations are much more intricate.

The fraction β of minority chains is assumed to be small ($\beta \ll 1$), and the average distance between them $(s/\beta)^{1/2}$ is large compared to their lateral size $K^{1/2}$. Here, we are using a mean-field approach and neglect swelling on the length scale of one blob. On the other hand, the majority chains are assumed to be strongly crowded. Thus, two inequalities have to be satisfied simultaneously: $\rho\beta K \ll 1$ and $\rho N \gg 1$. We now describe the conformation of a minority chain for three possible cases: $K = N$, $K < N$, and $K > N$.

1. Monodisperse Brush. If $K = N$, the standard analytical results discussed in detail in ref 8 apply. The density profile for the segments of the minority chain (which is now identical to the main chain) decreases parabolically with the distance from the grafting plane and goes to zero at the height

$$H = (8/\pi^2)^{1/3}\rho^{1/3}N \tag{1}$$

The density distribution for the free end position is

$$f(z_N) = Az_N(1 - (z_N/H)^2)^{1/2} \tag{2}$$

A being the normalization constant, which gives the average height of the free end and its root mean square (rms) fluctuation

$$\langle z_N\rangle = \frac{3\pi}{16}H \tag{3a}$$

$$\delta_{zN} \equiv (\langle z_N{}^2\rangle - \langle z_N\rangle^2)^{1/2} \approx 0.23H \tag{3b}$$

The average position and its fluctuation for each internal segment with number i ($i = 1, N$) are directly related to those of the end segment in a monodisperse brush:

$$\langle z_i\rangle = \sin\frac{\pi i}{2N}\langle z_N\rangle \tag{4a}$$

$$\delta z_i = \sin\frac{\pi i}{2N}\delta z_N \tag{4b}$$

2. Short Minority Chain. The case of $K < N$, i.e., the behavior of shorter chains inserted in a monodisperse brush, was discussed in refs 7 and 9. It was assumed that a minority chain experiences the self-consistent potential

$$U_N(z) = \frac{3\pi^2}{8N^2}(H^2 - z^2) \qquad 0 \le z \le H \tag{5}$$

which is due to the segment concentration of the main chains, and the change in the potential due to the foreign chain itself was neglected. The problem is now to find the conformation of an ideal chain consisting of $K < N$ segments in the external field $U_N(z)$.

The partition function $G(z',z|n)$ (integrated over the lateral coordinates x and y) for the chain with one end fixed at distance z' from the plane and the other end being at distance z satisfies the equation

$$-\frac{\partial G}{\partial n} = -\frac{1}{6}\frac{\partial^2 G}{\partial z^2} + U_N(z)G \tag{6}$$

subject to the initial condition $G(z',z|0) = \delta(z'-z)$ and the boundary condition at the impenetrable surface $G(z',0|n) = 0$.

Since as we shall see, for $K < N$, the average size of the minority chain is usually considerably smaller than H, we extend the potential field to $z \to \infty$ without affecting the problem (except for the case when K becomes very close to N). Equation 6 can be mapped onto the Schrodinger equation for the Green's function of a harmonic oscillator,

$$\frac{i}{\hbar}\frac{\partial G}{\partial t} = -\frac{\hbar^2}{2m}\frac{\partial^2 G}{\partial z^2} + \frac{1}{2}m\omega^2 z^2 G$$

by substituting $\hbar = 1$, $t = iN$, $m = 3$, and $\omega = i\pi/2N$. Note that the two Euclidean rotations, both in time and frequency complex planes, are involved. The solution of our polymer problem can be constructed from the quantum-mechanical result[10] by using the standard mirror image method to satisfy the boundary condition on the impenetrable plane:

$$G(z',z|K) = e^{-KU_0}\left(\frac{3}{N\sin(\pi K/2N)}\right)^{1/2} \times \exp\left\{-\frac{3\pi}{4N}(z^2+z'^2)\cot\left(\frac{\pi K}{2N}\right)\right\}\sinh\left(\frac{3\pi z z'}{2N\sin(\pi K/2N)}\right) \quad (7)$$

where $U_0 = U_N(0) = {}^3/_8({}^{\pi H}/_N)^2$. When the first segment is fixed at the plane $z' \to 0$, eq 7 reduces to

$$G(0,z|K) = Az\exp\left\{-\frac{3\pi\cot(\pi K/2N)}{4N}z^2\right\} \quad (8)$$

Here the prefactor A does not depend on z and is therefore not important for calculating averages. It is now straightforward to find the average height of the free end and its rms fluctuation

$$\langle z_K\rangle = \left[\frac{N}{3}\tan\left(\frac{\pi K}{2N}\right)\right]^{1/2} \cong \begin{cases}(\pi/6)^{1/2}K^{1/2} & K \ll N \\ (2N/3\pi)^{1/2}(1-K/N)^{-1/2} & 1-K/N \ll 1\end{cases} \quad (9a)$$

$$\delta z_K = \left(\frac{4}{\pi}-1\right)^{1/2}\langle z_K\rangle \quad (9b)$$

We now consider the average position and its fluctuation of an arbitrary ith segment of the chain $i = 1, K$. The calculation given in Appendix 1 yields

$$\langle z_i\rangle = b(i)\left(\frac{N\sin(\pi i/2N)\cos(\pi(K-i)/2N)}{3\cos(\pi K/2N)}\right)^{1/2} \quad (10a)$$

$$\delta z_i = c(i)\langle z_i\rangle \quad (10b)$$

where $b(i)$ and $c(i)$ are both weak functions of the segment number, i, with the following asymptotical values for the two ends of the chain:

$$b(i) = \begin{cases}4/\pi & \text{small } i \\ 1 & \text{large } i\end{cases} \quad (11)$$

$$c(i) = \begin{cases}(3\pi/8-1)^{1/2} & \text{small } i \\ (4/\pi-1)^{1/2} & \text{large } i\end{cases} \quad (12)$$

The crossover value of i dividing the two asymptotics is $i^* \sim K/2$, when the minority chain is considerably shorter than the main chains; or $i^* \sim N - K$, when the two contour lengths are close to each other: $N - K \ll N$.

The above formulas 9−12 are valid as long as they give values smaller than those for the main chains of the brush, eqs 1 and 3. For $K = N$, the chain size given by eq 9 diverges, since the Gaussian elasticity of the softest mode is completely canceled by the stretching external field. This is the result of the approximation whereupon the field was extended to infinity, while in a real brush the chain fluctuates only over the region where the field $U_N(z)$ exists, i.e. $0 \le z \le H$ (fluctuations beyond $z = H$ are asymptotically negligible). Both $\langle z_K\rangle$ and δz_K saturate at the values given by eqs 3a,b. The size fluctuations of a minority chain are always enhanced as compared to those in an ideal isolated coil. The range of validity for the approximation used is given by $\delta z_K^{\text{ideal}} \le \delta z_K \le \delta z_N$. Since the maximum increase in fluctuations achieved in a monodisperse brush is by a factor of $\rho^{1/3}N^{1/2}$, this range may be quite large.

3. Long Minority Chain: A Simple Approach. Since the stretching field produced by the concentration profile of the majority chains is just strong enough to cancel the elasticity of the N-segment chain, the more susceptible polymer with $K > N$ will be uncoiled and the "excess" $(K - N)$ segments will be pushed out of the brush, beyond the edge $z = H$. The long minority chain therefore acquires a flower conformation with a stretched stem and a coil-like crown (Figure 1). It is easy to show that the minimum of the mean-field free energy in the Newtonian strong-stretching limit (assumed in the analytical theories) corresponds to the conformation where the first N segments of the chain lie within the brush, while the $(K - N)$ end segments form a crown outside the brush. As a simple approximation, one can assume that the crown is an ideal coil attached to an impenetrable surface whose position coincides with the brush edge $z = H$. Then, the average position of the free end and its fluctuation are given by

$$\langle z_K\rangle = H + \left(\frac{\pi}{6}(K-N)\right)^{1/2} \quad (13a)$$

$$\delta z_K = \left(\frac{4-\pi}{6}(K-N)\right)^{1/2} \quad (13b)$$

The conformation of a minority chain with $K > N$ is not homogeneous, and therefore, the dependence of the position fluctuations on the segment number should be also described by two different branches. The first N segments belong to the stem whose end we assume to be fixed at distance H from the grafting surface, while the rest form a coil. For the stem segments inside the brush (see Appendix 1)

$$\langle z_i\rangle = H\sin\frac{\pi i}{2N} \qquad i \le N \quad (14a)$$

$$\delta z_i = \left(\frac{N}{3\pi}\sin\frac{\pi i}{N}\right)^{1/2} \qquad i \le N \quad (14b)$$

Assuming in the simplest approximation that the crown segments do not penetrate the brush, we use the familiar result for an isolated ideal chain near an impenetrable surface:

$$\langle z_i\rangle = H + \left(\frac{\pi}{6}(i-N)\right)^{1/2} \qquad i \ge N \quad (15a)$$

$$\delta z_i = \left(\frac{4-\pi}{6}(i-N)\right)^{1/2} \qquad i \ge N \quad (15b)$$

Here, we neglected the weak effect of the tail beyond the ith segment in order to keep the formulas as simple as possible. Note that the excluded volume effects in the crown are not taken into account by the version of the SCF method we use. The modification of eqs 15a,b to account for these effects at the level of the scaling approach is straightforward:

$$\langle z_i\rangle \approx H + \text{const}(i-N)^{\nu}$$

$$\delta z_i \approx \text{const}(i-N)^{\nu}$$

Of course, the position of the Nth segment actually fluctuates, and the segments of the crown can somewhat penetrate the brush which is especially important when the minority chains are only slightly longer. However, we expect the picture to be reasonable for asymptotically

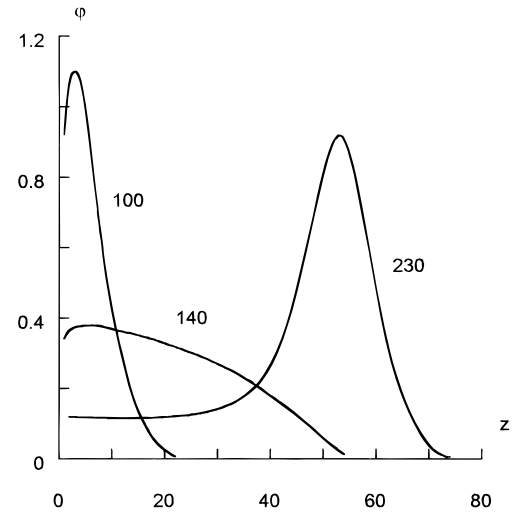

Figure 2. Minority chain segment density profiles. The brush parameters are $N = 140$, $\rho = 0.1$. The minority chain length K is shown in the picture.

long chains. A more refined consideration of fluctuation effects is given in section IV.

Summing up all the analytical results, one can say that the minority chain can take three different types of conformation depending on its molecular mass: a slightly deformed coil for $K < N$; a strongly stretched, strongly fluctuating chain for $K = N$; and a flower with a stretched weakly fluctuating stem and a coil-like crown for $K > N$. As eqs 9 and 13b show, the size of the shorter chain and the fluctuations of the free end for both shorter and longer minority chains in a monodisperse brush do not depend on the brush density. The grafting density ρ enters only in the brush thickness H and controls the fluctuations only when the lengths of the minority and the main chains are very close.

III. Comparison with Numerical Results

The density profiles of monodisperse brushes with $N = 30$, 60, 100, 140, 200, and 500 and grafting densities $\rho = 0.03$ and 0.1 were calculated for chains on a simple cubic lattice within the standard self-consistent field approach known as the Scheutjens−Fleer model. (The numerical procedure and the limitations of the approach are discussed in refs 3 and 11.) Then, the properties of a minority chain in the calculated self-consistent field were obtained. Three types of conformations acquired by minority chains of different lengths are clearly shown by the segment density profiles (Figure 2). Here, the brush parameters are $N = 140$ and $\rho = 0.1$. A shorter chain with $K = 100$ forms a weakly deformed coil that stays relatively close to the grafting plane. A chain identical to the main chain $K = N = 140$ fluctuates strongly throughout the brush thickness and reproduces the parabolic density profile. A longer chain, $K = 180$, is strongly heterogeneous. The stem inside the brush has an almost constant density profile, while the crown has the conformation with the density profile close to that of a Gaussian coil.

Figure 3a,b shows the dependence of the average height $\langle z_K \rangle$ and its fluctuation δz_K for a minority chain as a function of the number of segments, K. The chain is inserted into a monodisperse brush with $N = 100$ and $\rho = 0.1$. The brush thickness calculated according to eq 1 is $H = 38.7$ and is shown by a dotted line. It is clear that the simple analytical formulas 3−9 (dashed lines 1 and 2) give a fairly good description of the

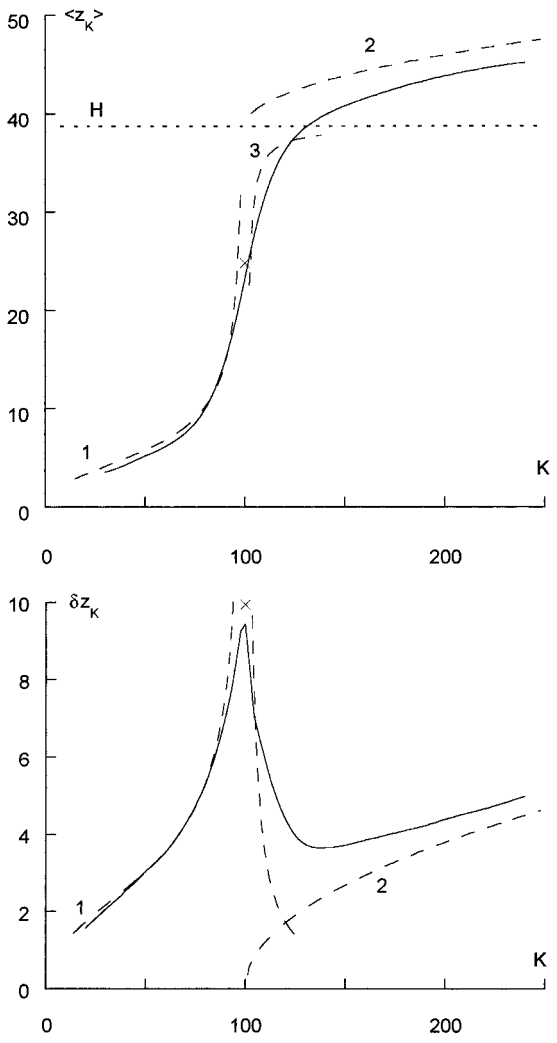

Figure 3. (a) The average height of the minority chain free end *vs* its contour length, K. The brush parameters are $N = 100$, $\rho = 0.1$. The brush thickness is shown by the dotted line, the average height of a majority chain free end by the cross. Broken line curves 1, 2, and 3 represent three asymptotic regimes given by eqs 9a, 13a, and 17a, respectively. (b) The same for the rms fluctuation of the height of the minority chain free end. Broken line curves 1, 2, and 3 are calculated according to eqs 9b, 13b, and 17b, respectively.

numerical results. The accuracy is especially good for shorter chains. For long chains having a well-formed flower conformation, the average height of the free end follows rather closely the analytical curve 2 but is consistently shifted to lower values. Qualitatively, this means that the brush becomes effectively impenetrable at a height somewhat lower than the one given by eq 1. The case of K being just slightly larger than N is not treated properly within the simple approach presented above, which does not describe a smooth but rapid increase in $\langle z_K \rangle$ in the range $\langle z_N \rangle \le \langle z_K \rangle \le H$. Analytical curve 3 based on the incorporation of fluctuation effects is derived in the next section.

The dependence of the minority chain end fluctuations on the contour length (Figure 3b) clearly displays three regimes, while the analytical formulas given so far cover only two of them (dashed curves 1 and 2). The enhanced coil fluctuations for $K < N$ are well described by eqs 9a,b. When K is considerably larger than N, the contribution of the crown (eq 13b) gives a reasonable estimate of the chain end fluctuation. For K slightly larger than N, the simplistic approach fails. An improved analytical description covering the third regime

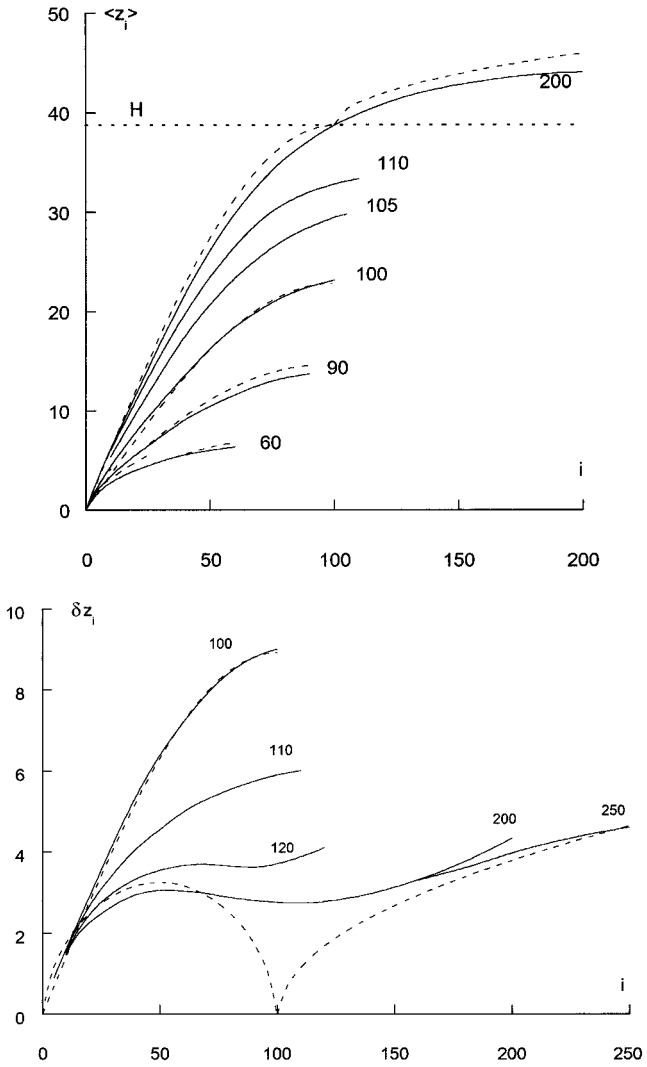

Figure 4. (a) The average height of the internal *i*th segment for minority chains of different length *K* (shown on the curves) *vs* its number, *i*, counted from the grafting site. The brush parameters are $N = 100$, $\rho = 0.1$. The brush thickness is shown by the dotted line. Broken line curves for $K = 60$ and 90 are calculated from eqs 10a and 11, for $K = N = 100$ from eq 4a, and $K = 200$ from eqs 14a and 15a. (b) The same for the rms height fluctuation of the *i*th segment of the minority chain. Broken line curves represent eq 4b for $K = N$ and the asymptotic formulas 14b and 15b for $K \gg N$.

(curve 3) is given in the next section.

Detailed Conformation of the Minority Chain. Figure 4a shows the average position for each monomer of different minority chains as a function of the monomer number, *i*, counted from the grafted end. Minority chains are inserted in a brush with $N = 100$ and $\rho = 0.1$. It is clear that for shorter minority chains and for the marginal case $K = N$ the analytical description compares very well to the numerical results. For chains slightly longer than *N*, the discrepancy is considerable. For a very long minority chain ($K = 200$), eqs 14a and 15a match the calculated results rather well. In particular, the mean height of the *N*th segment is indeed very close to the calculated value of *H*.

The position fluctuations for various monomers of shorter and marginal ($K = N$) chains are in a good agreement with the analytical predictions, similar to what is displayed in Figure 4a (in fact, in this regime $\langle z_i \rangle$ and δz_i differ only by a constant numerical factor). It is the case of longer chains where the simplistic approach (eqs 14b and 15b) fails, as displayed in Figure 4b. Once again, the case of *K* slightly larger than *N* is the worst, the existing effect not being covered at all. For very long minority chains $K \gg N$ having the flower conformation, the analytical curve does reflect some essential qualitative features of the numerical results. It is clear, though, that the position of the *N*th segment is not fixed at height *H* but rather fluctuates about it with a finite amplitude.

IV. Fluctuation Effects

Position of the Chain End. The picture of a longer minority chain with its *N*th segment fixed on the brush edge $z = H$ is obviously incorrect for the case when *K* is only slightly larger than *N*; see Figure 3a. The effect of adding a few extra ($K - N$) segments is very pronounced. The reason is that with the increase in $K - N$ the free end position probability density is quickly changing in such a way that the end segment is being pushed toward the brush edge. Note that in a monodisperse brush the width of the probability density is on the order of the brush thickness $H \sim N$, while the characteristic distance by which the end segment extends outside the brush profile is much smaller:[2] the fringe thickness, d_{fringe}, is only of order $N^{1/3}$. Naturally, if the presumed size of the coil-like crown $(K - N)^{1/2}$ for a longer minority chain is also on the order of or smaller than d_{fringe}, one can neglect the probability of the end segment appearing beyond the brush edge $z = H$. Inside the brush, for $z_K < H$, eq 8 for the free end density still applies:

$$f(z_K) = Az_K \exp\left\{-\frac{3\pi \cot(\pi K/2N)}{4N} z_K^2\right\} \sim \exp\left(\frac{3\pi^2(K-N)}{8N^2} z_K^2\right) \quad (16)$$

but at $z_K = H$ the function should be truncated. (A more careful consideration is given in Appendix 2.) Calculating the average height and its fluctuation, one obtains

$$\langle z_K \rangle = H - \frac{4N^2}{3\pi^2 H(K-N)} \quad (17a)$$

$$\delta z_K = \frac{4N^2}{3\pi^2 H(K-N)} \quad (17b)$$

The validity of these asymptotic formulas is subject to two simultaneous conditions: $\delta z_K \gg d_{\text{fringe}} \sim N^{1/3}\rho^{-1/9}$ and $K - N \gg 1$. For $K - N \sim N^{2/3}\rho^{-2/9}$ the width of the probability density given by eq 16 decreases to the extent that it becomes comparable to d_{fringe}. At this point, the fluctuations outside the brush edge are not negligible any more, and the flower conformation emerges. Figure 3b demonstrates the existence of three regimes: (1) the enhanced coil fluctuations for $K < N$ given by eqs 9a,b, (2) the regime dominated by the flower conformation for large $K - N$ (eq 13b), and (3) the intermediate regime for relatively small $K - N$, where fluctuations display a very sharp decrease with the increase in *K* that has just been described (eq 17b).

Stem Fluctuations. The somewhat speculative considerations of the previous subsection are put on a firmer basis by the derivation of the asymptotic form of the probability density for the position of the *N*th segment presented in the Appendix 2. The flower conformation is inhomogeneous: On average, it is the

Nth segment that separates the stretched stem of height H, and the coiled crown. One can identify two regimes:

(1) If the chain is just slightly longer than the majority chains, the probability density distribution is strongly asymmetric. The characteristic size of the fluctuation outward is $\delta z_N^{\text{out}} \sim \rho^{-1/9}N^{1/3}$, which is of course on the order of the fringe thickness, while the characteristic size of the fluctuation inward is $\delta z_N^{\text{in}} = 4N^2/[3\pi^2 H(K - N)]$, which is $\sim N^1$ when the difference $(K - N)$ is on the order of unity. Under the condition $K - N \ll \rho^{-2/9}N^{2/3}$, the inward fluctuation is larger and dominates the total effect both in terms of the average position of the Nth segment and its rms fluctuation:

$$\langle z_N \rangle = H - \frac{4N^2}{3\pi^2 H(K - N)} \tag{18a}$$

$$\delta z_N = \frac{4N^2}{3\pi^2 H(K - N)} \tag{18b}$$

It is remarkable that, in the asymptotic regime discussed here, the density of the Nth segment is exactly the same as the density of the free end (Kth segment) given by eq 16. The result would be strictly correct if the field were parabolic everywhere (see Appendix 2).

(2) In a well-developed flower conformation ($K - N \gg \rho^{-2/9}N^{2/3}$), the probability density is practically symmetric about $z_N = H$. The magnitude of the fluctuation for the position of the Nth segment as calculated in Appendix 2 is given by

$$\delta z_N \approx 0.36\rho^{-1/9}N^{1/3} \tag{19}$$

The analytical predictions for both regimes are verified by computer calculation results. The hyperbolic dependence of $\langle z_N \rangle$ and δz_N on $(K - N)$ is supported by the computer calculations reasonably well (Figure 3a,b). Some discrepancies are probably due to the fact that the partition function (7) does not take into account small corrections to the parabolic shape that exist in the true self-consistent potential.[12] The fluctuations in a well-developed flower obey the scaling of eq 19 excellently; see Figure 5. Even the numerical prefactor in eq 19 compares rather well with the best fit value of 0.46 for the numerical data.

V. Coil-to-Flower Transition

We have seen that, as the contour length of the minority chain is increased, its conformation changes from a random coil to a flower. The transition from one type of conformation to another occurs as the number of segments of the minority chain changes within a very narrow range around N. The two types of conformation differ qualitatively. In the coiled state, although the coil is somewhat deformed by the molecular field of the brush, both the average end height and its fluctuation are proportional to $K^{1/2}$, and the stretching parameter defined as $\langle z_K \rangle/K \sim K^{-1/2}$ tends to zero as $K \to \infty$. The conformation of a well-developed flower is inhomogeneous. The crown is still a random coil, but the stem is strongly stretched and fluctuates only weakly: $\langle z_N \rangle \cong H \sim N$, $\delta z_N \sim N^{1/3}$. In the middle of the transition when the contour length of the minority chain exactly equals N, the chain is stretched and at the same time strongly fluctuates: $\langle z_N \rangle \sim \delta z_N \sim H$.

This picture can be treated quite naturally in the framework of phase transition theory. It is clear that the most dramatic changes occur in the stretching parameter of that part of the chain which stays inside of the brush profile. This comprises the whole minority chain in the case of $K < N$, and the N-segment stem in the case of a longer minority chain where $K > N$. It should not be totally surprising that the stretching parameter for the inside part of the minority chain makes a good choice to serve as an order parameter:

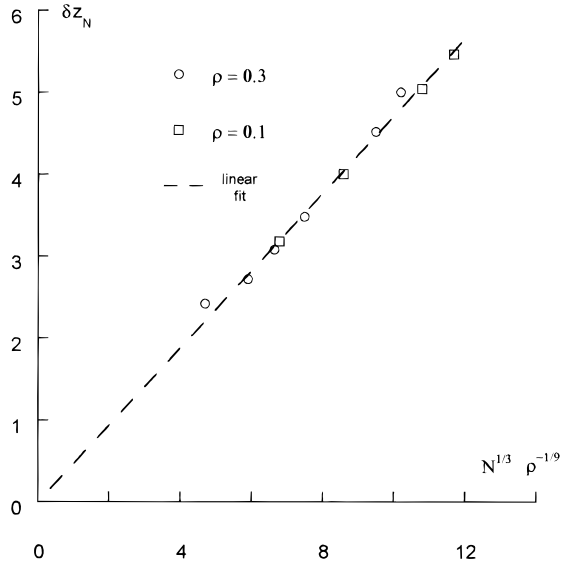

Figure 5. Stem fluctuations for long minority chains in a well-developed flower-like conformation *vs* the scaling parameter $\rho^{-1/9}N^{1/3}$. The broken line gives the linear fit as suggested by eq 29. The values of the brush grafting density are shown in the figure.

$$\xi = \begin{cases} z_K/K & K \le N \\ z_N/N & K \ge N \end{cases} \tag{20}$$

Note that the order parameter is defined as an instantaneous variable and is allowed to fluctuate. Figure 6a displays the dependence of the averaged order parameter on the contour length ratio K/N. It is clear that the curves become steeper as the brush thickness increases, and in the thermodynamic limit $K,N \to \infty$ one arrives at a step function. In this limit, the order parameter has a finite jump from $\langle \xi \rangle = 0$ to $\langle \xi \rangle = 3/8(\rho/\pi)^{1/3}$ at the point $K/N = 1$. The initial decrease in $\langle \xi \rangle$ at small values of K/N is just a property of an ideal coil, $\langle \xi \rangle \sim K^{-1/2}$.

For ideal Gaussian coils, the mean-square fluctuation of the stretching parameter is $(\delta\xi)^2 = (\delta z_N/N)^2 \sim N^{-1}$, and therefore $N(\delta\xi)^2$ is a constant independent of the contour length of the chain. Taking this as an appropriate normalization, we display in Figure 6b the fluctuation of the order parameter for a minority chain in the brush. For shorter minority chains ($K < N$), the value of $K(\delta\xi)^2$ is described very well by the analytical expressions of eqs 9a,b. For $K \ll N$, the curve tends to a constant value $K(\delta\xi)^2 = (4 - \pi)/6 \approx 0.14$, characteristic of an ideal coil near an impenetrable planar surface. As the contour length of the minority chain increases, the fluctuations display anomalous growth. When K becomes close to N, this growth is described by a power law $K(\delta\xi)^2 \sim \lambda^{-1}$, where $\lambda = 1 - K/N$ is the deviation from the transition point.[7] The picture is characteristic of critical behavior near the point of a second-order phase transition. In the language of critical phenomena, the value of index γ describing the divergence of susceptiblity is $\gamma = 1$, which is the mean-field value given by the Landau theory.

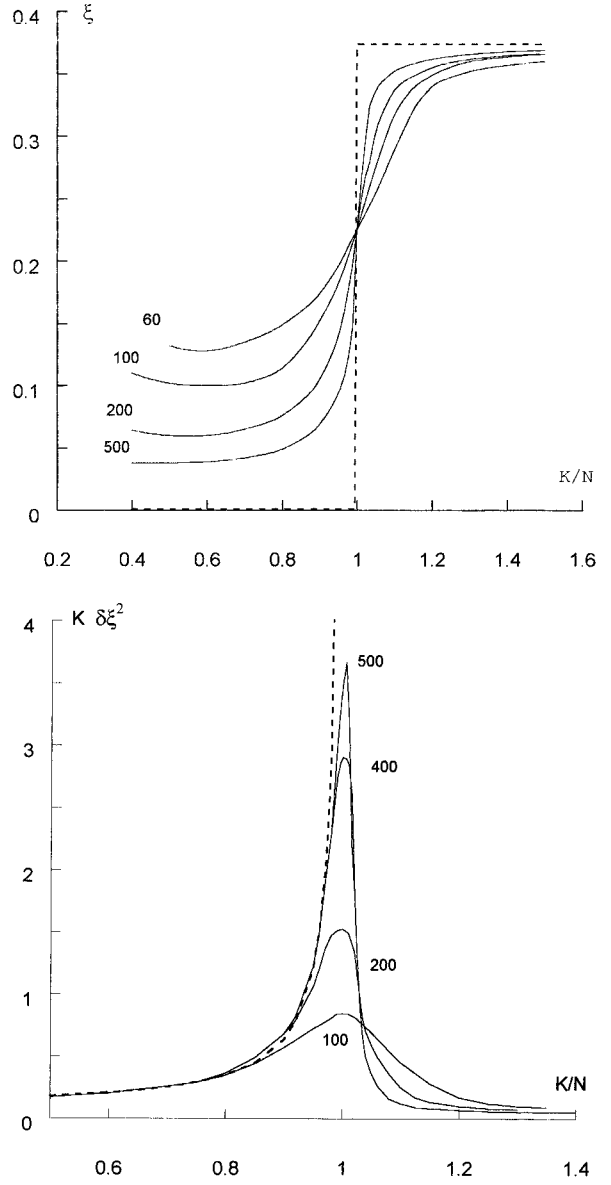

Figure 6. (a) The dependence of the average order parameter (the stretching degree) for minority chains of K segments surrounded by majority chains of N segments, on their contour length ratio K/N. Numbers on the curves refer to different values of N. The grafting density is $\rho = 0.1$. The broken line gives the asymptotic step function in the $K \to \infty$, $N \to \infty$ limit. (b) The same for reduced average squared fluctuation of the order parameter. The dashed line plots eq 9b.

If the transition point is approached from above ($K > N$), the order parameter fluctuations also grow according to a power law (see eq 18b) but with a different exponent, $\gamma = 2$: $N(\delta\xi)^2 \sim |\lambda|^{-2}$. The analytical predictions for the fluctuation growth in the vicinity of the transition point are checked against numerical calculations in Figure 7. Two different slopes on the log−log plot of $K(\delta\xi)^2$ versus λ show clearly a marked asymmetry of the fluctuation behavior. The power laws represent only certain asymptotic regimes, and there are corrections both away from the transition point and very close to it, where saturation comes into play. The predicted values of the critical index $\gamma = 1$ (for $K < N$), and $\gamma = 2$ (for $K > N$) compare reasonably well to the numerical data in the regime where corrections are not important. For small systems, the asymptotic power-law regime may be too narrow to be clearly detected.

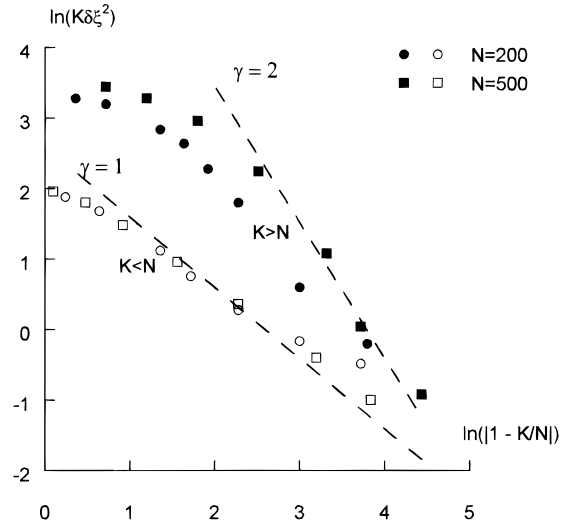

Figure 7. log−log plot of the reduced average squared fluctuation of the order parameter *vs* the relative contour length difference $1 - K/N$. Dashed straight lines correspond to critical behavior with two different values of index γ.

According to the standard classification of phase transitions in a first-order transition, the order parameter changes jumpwise while the susceptibility is a smooth function of the governing parameter except at the transition point itself, where it is mathematically ill-defined. In a second-order phase transition, the order parameter changes smoothly, and the susceptibility displays power-law (or logarithmic) divergence at the critical point. Our system combines the features of both types of phase transitions: the order parameter has a finite jump and at the same time a power-law anomalous fluctuation growth on the approach of the transition point. The same type of behavior is displayed by another polymeric system: a macromolecule adsorbing on a planar surface in the presence of a constant force applied to its end.[12]

From the viewpoint of the Landau theory,[13] the transition in question should be treated rather as a second-order transition, since the order parameter probability density remains unimodal for all values of the governing parameter, λ, and the transition goes through anomalous broadening of the probability density function. Figure 6b clearly shows that the width of the fluctuation growth curve does not narrow down with the increase in the size of the system and remains finite in the $K,N \to \infty$ limit. Conversely, classical first-order transitions do not have strong pretransitional effects in a finite vicinity of the transition point. A finite jump in the order parameter for the transition discussed is due to the fact that in the $K,N \to \infty$ limit the free energy as a function of the order parameter differs from what the Landau theory postulates: it contains the quadratic term but none of the higher powers[7] that would normally define the transition type. Instead, an additional nonanalytic term of a different form is dominant at the transition point. It was shown in ref 7 that this feature is not related to the Gaussian approximation but remains valid for chains of finite extensibility.

One more peculiarity of the transition under consideration is that the governing parameter does not have the meaning of temperature, or interaction strength, but the ratio of contour lengths K/N for the minority and majority chains.

VI. Discussion

A minority chain in a monodisperse brush can take three types of conformations depending on its contour length relative to that of a majority chain. Shorter chains form slightly deformed coils. Longer chains acquire an inhomogeneous flower-like conformation. The transition between these two conformations goes through an intermediate conformation that is strongly stretched and strongly fluctuating at the same time. The transition, governed by the change in the contour length ratio K/N, has certain features of a phase transition. A very small change in the contour length of a minority chain (relative to N) may change its conformation dramatically.

Solvent Quality Effect. So far, in our discussion we have assumed that the brush is immersed in a good solvent. The brush affects the conformation of a minority chain through the averaged molecular field, described by the parabolic potential (eq 5). With the change in the solvent quality, it is only the brush thickness that changes, but the functional form of the self-consistent potential remains the same.[14] It follows immediately that the three types of conformations described above, and the character of the transition between them, should refer equally well to the system in a Θ-solvent. The case of a poor solvent is more complicated due to surface tension effects coming into play. One can envision that the picture of the long chain conformation, as well as the character of the stem fluctuation, will be different.

Polydispersity Effect. Consider now a brush formed originally by polydisperse macromolecules with a relatively broad continuous molecular mass distribution. In this case the degree of stretching (the order parameter introduced above) of a chain in the brush is a smooth function of its contour length.[9] Of course, admixed macromolecules that are considerably shorter than any of the brush-forming chains will still be coiled, while those considerably longer will take a flower conformation. However, the transition between these conformations will be gradual, without any features of a phase transition. This difference may not be easily detected experimentally, especially when static quantities are measured. For a monodisperse brush, the most dramatic effects refer to fluctuations rather than to average heights, density profiles, etc. Strong changes in fluctuation magnitudes should reveal themselves in dynamic behavior.

Relaxation Phenomena. The large scale end-to-end distance relaxation time scales as $\tau \sim \zeta \langle \delta z_K^2 \rangle$, where ζ is the global friction coefficient. A minority chain shorter or just slightly longer than a main chain is practically entirely inside the brush where the concentration effects lead to screening of hydrodynamic interactions. Therefore, its friction coefficient is proportional to the number of hydrodynamic blobs, or $\zeta \sim K$. Referring the relaxation time of the minority chain to that of an isolated ideal free-draining coil, one obtains $\tau_{\text{minor}}/\tau_{\text{Rouse}} = \text{const}(\langle \delta z_K^2 \rangle / K)$. This ratio as a function of the relative contour length of the minority chain is qualitatively similar to what is displayed in Figure 3b. It is clear that the relaxation time is a strongly nonmonotonous function of the molecular weight. Short minority chains obey the Rouse scaling $\tau \sim K^2$. With K approaching N, the relaxation slows down anomalously due to the pretransitional fluctuation growth, to become $\tau \sim N^3$ in a monodisperse brush. For larger values of K, τ first decreases very sharply down to the value $\tau \sim N^{5/3}$. This happens when the stem fluctuation magnitude becomes comparable to crown size: $\langle \delta z_K^2 \rangle \sim \langle \delta z_N^2 \rangle \sim N^{2/3}$. Eventually, for a very long minority chain, the end-to-end distance relaxation should be determined by that of the crown, which gives $\tau \sim (K - N)^{3\nu}$ (for a realistic chain in solution) or $\tau \sim (K - N)^{2\nu+1}$ (for a free-draining model), ν being the standard Flory index ($\nu = 0.59$ for a good solvent and $\nu = 0.5$ for Θ-conditions). The stem relaxation in this case should depend only on the brush properties and not on the molecular mass of the minority chain $\tau_{\text{stem}} \sim N^{5/3}$.

It would be very interesting to check the predicted effects, especially since they seem to be so strong. This could probably be done most naturally by direct computer simulations of more realistic multichain models.[15,16] An accurate experimental verification might be difficult, since it first requires preparing a monodisperse brush and then introducing a well-characterized minority component and measuring its properties. Perhaps, using deuterated chains, one could observe the change in the density profiles for the minority chains of different contour length, as shown in Figure 1.

Acknowledgment. This work was supported by the Russian Foundation for the Basic Research Grants 94-03-09607 and 96-03-33862.

Appendix 1

Average Position and Fluctuation of the *i*th Segment, *i* < *N*. If the nonanchored end of a minority chain can fluctuate over the brush thickness, the nonnormalized probability density for the height of the ith segment, $f(z_i)$, can be written as

$$f(z_i) = G(0,z_i|i) \int_0^H G(z_i,z|K-i)\, \mathrm{d}z \qquad \text{(A1)}$$

where the partition functions of the two tails (1, i) and (i, K) are given by eqs 7 and 8. The (l,m) notation denotes the subchain starting from segment l and ending with segment m. Extending the integration limit to infinity, one obtains:

$$f(z_i) = Az_i\left\{\mathrm{erfc}\left(-z_i\sqrt{\frac{3\psi}{\sin(2(K-i)\psi)}}\right) - \mathrm{erfc}\left(z_i\sqrt{\frac{3\psi}{\sin(2(K-i)\psi)}}\right)\right\} \times \exp\left(-\frac{3\psi\cos(K\psi)}{2\sin(i\psi)\cos((K-i)\psi)}z_i^2\right) \qquad \text{(A2)}$$

where $\psi = \pi/2N$. The expression in parentheses has two simple asymptotics:

$$\text{const } z_i, \text{ if } \quad z_i\sqrt{\frac{3\psi}{\sin 2((K-i)\psi)}} \ll 1$$

$$\text{and const, if } \quad z_i\sqrt{\frac{3\psi}{\sin 2((K-i)\psi)}} \gg 1$$

Hence, asymptotical analytical expressions for the average positions and their fluctuations can be obtained. The first set,

$$\langle z_i \rangle = \frac{4}{\pi}\left(\frac{N\sin(i\psi)\cos(K-i)\psi)}{3\cos(K\psi)}\right)^{1/2} \qquad \text{(A3)}$$

$$\delta z_i = \left(\frac{3\pi}{8} - 1\right)^{1/2} \langle z_i \rangle \tag{A4}$$

is valid if the main contribution to the averages comes from the region

$$z_i \ll \sqrt{\frac{2N \sin 2((K-i)\psi)}{3\pi}}$$

The second set differs only by numerical prefactors

$$\langle z_i \rangle = \left(\frac{N \sin(i\psi) \cos(K-i)\psi)}{3 \cos(K\psi)}\right)^{1/2} \tag{A5}$$

$$\delta z_i = \left(\frac{4}{\pi} - 1\right)^{1/2} \langle z_i \rangle \tag{A6}$$

and is valid when the opposite inequality is satisfied. In simple words, for the segments near the grafted end of the chain, the repulsive effect of the plane is stronger. The marginal value of the segment number, i^*, separating the two regimes is obtained from

$$\langle z_i^* \rangle \sim \sqrt{\frac{2N \sin 2((K - i^*)\psi)}{3\pi}} \tag{A7}$$

which gives $i^* \sim K - i^*$, or $i^* \sim K/2$, when $\lambda = (N - K)/N$ is on the order of unity, and $i^* \sim N - K$, when $\lambda \ll 1$.

When considering the stem of the long minority chain in the simplest approximation, the Nth segment is assumed to be fixed at height H. Then, eq A1 should be modified

$$f(z_i) = G(0,z_i|i)\, G(z_i,H|K-i) \tag{A8}$$

to give

$$f(z_i) = Az_i \exp\left\{-\frac{3\psi}{\sin(2i\psi)}(z - H \sin(i\psi))^2\right\} \tag{A9}$$

Neglecting the repulsive effect of the grafting plane reflected in the linear factor in eq A9, one arrives at

$$\langle z_i \rangle = H \sin i\psi \tag{A10}$$

$$\delta z_i = (N \sin (2i\psi))^{1/2} \tag{A11}$$

where again $\psi = \pi/2N$.

Appendix 2

Probability Density for the Position of the Nth Segment in a Longer Chain. The non-normalized probability density for the Nth segment can be written as

$$f(z_N) = G(0,z_N|N) \int_0^\infty G(z_N,z|K-N)\, \mathrm{d}z \tag{A12}$$

We are going to write down the asymptotics of $f(z_N)$ for two cases $z_N > H$ and $z_N < H$ separately.

I. If $z_N > H$, the (N, K) subchain is, to a good approximation, completely outside the brush, and we neglect the dependence of its partition function $\int_0^\infty G(z_N,z|K-N)\, \mathrm{d}z$ on z_N in this region. Omitting the constant factors that are not important for calculating averages, the partition function of the $(1, N)$ stem can be written as

$$G(0,z_N|N) = \int_0^N G_{\mathrm{parab}}(0,H|N-n)\, G_0(H,z_N|n)\, \mathrm{d}n = \int_0^N \exp\left\{-\frac{3\psi}{2}H^2 \cot((N-n)\psi) - U_0(N-n) - \frac{3(z_N - H)^2}{2n}\right\} \mathrm{d}n \tag{A13}$$

where $\psi = \pi/2N$. Here, G_{parab} refers to the $(1, N - n)$ subchain which experiences the parabolic molecular field, while G_0 refers to the last n segments which are outside the brush where the molecular field is absent. Expanding $\cot((N - n)\psi) = \tan(\pi n/2N) \cong \pi n/2N + 1/3 (\pi n/2N)^3$ for $n/N \ll 1$ and recollecting that $U_0 = (3\pi^2H^2)/(8N^2)$, one can perform the integration in eq A13 asymptotically:

$$f(z_N) \approx \exp(\pi N^{-1} H^{1/2} (z_N - H)^{3/2}) \qquad z_N > H \tag{A14}$$

Here, we omitted the additional power function of $(z_N - H)$ appearing from the steepest descent integration method as an artifact due to simplification of the true self-consistent potential: it is obvious that at $z_N = H$ the true partition function should be finite and nonzero. The result of eq A14 was first obtained by Milner (see ref 2) when considering the fringe of a monodisperse brush.

II. The case $z_N < H$ should be in turn subdivided into two parts:

(1) Provided the $(K - N, K)$ subchain is short enough to be practically completely within the brush,

$$f(z_N) \approx G_{\mathrm{parab}}(0,z_N|N) \int_0^\infty G_{\mathrm{parab}}(z_N,z|K-N)\, \mathrm{d}z$$

and eq A2 applies with $i=N$

$$f(z_N) \approx \exp\left(-\frac{3\psi \cos(K\psi)}{2 \sin(N\psi) \cos((K-N)\psi)} z_i^2\right) = \exp\left(\frac{3\pi \tan(\pi(K-N)/2N)}{4N} z_i^2\right) \tag{A15}$$

Here, we have used $\sin(N\psi) = \sin(\pi/2) = 1$ and $\cos(K\psi) = \cos(\pi K/2N) = -\sin(\pi(K - N)/2N)$. Of course, eq A15 is applicable only for $z_N < H$. It is remarkable that the distribution density for the Nth segment is exactly the same as that for the free end (Kth segment) given by eq 17 of the present paper. The result would be strictly correct if the field were parabolic everywhere.

(2) If the tail comprising the last $(K - N)$ segments is not entirely within the brush, its partition function could be written as

$$\int_0^\infty \mathrm{d}z\, G(z_N,z|K-N) \approx \int_0^{K-N} \mathrm{d}n\, G_{\mathrm{parab}}(z_N,H|n) \int_H^\infty \mathrm{d}z\, G_0(H,z|K-N-n) \tag{A16}$$

We have assumed here that the $(K - N - n)$th segment is fixed at the edge of the brush, so that the partition function of the $(K - N - n, K)$ subchain lying predominantly outside the brush is well approximated by that of an isolated coil. The partition function of the $(N, N$

$+ n$) subchain is taken as if the parabolic field were infinite. For this approximation to be consistent, the position of the $(N + n)$th segment should satisfy the condition $\langle z_{N+n}\rangle \leq H$. Performing simple averaging with the probability density (eq 9) one obtains $\langle z_{N+n}\rangle = z_N(\cos n\psi)^{-1}$. Hence, the upper limit of integration over n in eq A16 should be changed to $n^* = \psi^{-1} \arccos(z_N/H) \approx 2^{1/2}\psi^{-1}(1 - z_N/H)^{1/2}$. Performing the asymptotic integration in the vicinity of the maximum of the exponent and omitting all the weaker nonexponential functions of $(H - z_N)$ including the one coming from the partition function of the tail outside the brush, we arrive at

$$G(0,z_N|K) \approx A \exp(9\pi 2^{-5/2} N^{-1} H^{1/2}(z_N - H)^{3/2}) \qquad z_N < H \tag{A17}$$

The inside branch of the distribution density (eq A17) has the same form as the outside branch (eq A14) except for a slightly different numerical coefficient in the exponent. The important qualitative fact is that the distribution density can never develop strong asymmetry about the point $z_N = H$, which is confirmed by computer calculations.

Calculating the average fluctuation of the Nth segment for the flower conformation with the density given by eqs A14, A17, and 1, we obtain

$$\delta z_N \approx 0.36\rho^{-1/9} N^{1/3} \tag{A18}$$

References and Notes

(1) Halperin, A.; Tirrel, M.; Lodge, T. P. *Adv. Polym. Sci.* **1991**, *100*, 31.
(2) Milner, S. T. *Science* **1991**, *251*, 905.
(3) Fleer, G. J.; Cohen Stuart, M. A.; Scheutjens, J. M. H. M.; Cosgrove, T.; Vincent, B. *Polymers at Interfaces*; Chapman and Hall: London, 1993.
(4) *Long and Short Chains at Interfaces*; Dailland, J. et al., Ed.; Editions Frontieres: France, 1995.
(5) Milner, S. T.; Witten, T. A.; Cates, M. E. *Macromolecules* **1989**, *22*, 853.
(6) Birshtein, T. M.; Lyatskaya, Yu. V.; Zhulina, E. B. *Polymr* **1990**, *31*, 2185.
(7) Klushin, L. I.; Skvortsov, A. M. *Macromolecules* **1991**, *24*, 1549.
(8) Lai, P.-I.; Zhulina, E. B. *J. Phys. II* **1992**, *2*, 547.
(9) Klushin, L. I.; Skvortsov, A. M. *Macromolecules* **1992**, *25*, 3443.
(10) Feynman, R. P.; Hibbs, A. R. *Quantum Mechanics and Path Integrals*; McGraw-Hill: London, 1965.
(11) Skvortsov, A. M.; Pavlushkov, I. V.; Gorbunov, A. A. *Polym. Sci. USSR* **1988**, *30*, 487.
(12) Gorbunov, A. A.; Skvortsov, A. M. *J. Chem. Phys.* **1993**, *98*, 5961.
(13) Landau, L. D.; Lifshits, E. M. *Statistical Physics*; Pergamon Press: New York, 1973.
(14) Zhulina, E. B.; Borisov, O. V.; Priamitsyn, V. A.; Birshtein, T. M. *Macromolecules* **1991**, *24*, 140.
(15) Murat, M.; Grest, G. S. *Macromolecules* **1989**, *22*, 4054.
(16) Lai, P.-I.; Binder, K. *J. Chem. Phys.* **1991**, *95*, 9288.

MA961111E